

# Mn(II) and VO(IV) Schiff base complexes encapsulated in nanocavities of zeolite-Y: catalytic activity toward oxidation of alkenes and reduction of aldehydes

Saeed Rayati<sup>1</sup> · Saeedeh Shokoohi<sup>1</sup> · Elaheh Bohloulbandi<sup>1</sup>

Received: 3 January 2016 / Accepted: 13 June 2016 / Published online: 20 June 2016  
© Iranian Chemical Society 2016

**Abstract** Oxovanadium(IV) and manganese(II) complexes of two Schiff base ligands, bis(2,4-dihydroxyacetophenone)-1,2-propandiimine ( $H_2L_1$ ) and bis(2,4-dihydroxyacetophenone)-ethylenediimine ( $H_2L_2$ ) were synthesized and characterized. The encapsulation of these complexes in the nanocavities of zeolite-Y was achieved by a flexible ligand method. The prepared heterogeneous catalysts have been characterized by FTIR, NMR and atomic absorption spectroscopy, X-ray diffraction patterns, scanning electron microscopy and BET. The catalytic activities of the encapsulated complexes were studied in the oxidation of alkenes with  $H_2O_2$  and the reduction of aldehydes with  $NaBH_4$ . In most cases, the manganese (II) complexes ( $MnL_1$ -Y,  $MnL_2$ -Y) showed better activity than the oxovanadium (IV) complexes ( $VO L_1$ -Y,  $VO L_2$ -Y) in both oxidation of alkenes and reduction of aldehydes. The catalytic activity of the recovered catalysts was compared with the fresh ones.

**Keywords** Zeolite · Heterogeneous catalyst · Schiff base · Nanocavity · Oxidation · Reduction

## Introduction

Zeolites are attractive materials for encapsulation of transition metal complexes, organic dyes, polymers and organometallic compounds within their voids [1, 2]. The zeolite-encapsulated transition metal complexes of Schiff

base ligands are well known to mimic the catalytic cycle of cytochrome P-450 and have attracted research interest in recent years [3, 4]. Encapsulated metallomacrocycles in the nanopores of zeolite-Y combine the advantages of homo- and heterocatalytic systems. These nanocomposite materials have been extensively used as biomimetic heterogeneous catalysts for oxidation reactions with a variety of oxidants [5–8] and reduction reactions with sodium borohydride [9–13].

We have developed many catalytic systems using transition metal complexes of Schiff base ligands for various oxidative chemical transformations [5, 14–16]. In comparison with the application of transition metal Schiff base complexes as oxidative catalysts, their ability to reduction reactions has received considerably less attention in organic synthesis [12, 13]. As an ongoing effort to emphasize the role of transition metal complexes of Schiff base ligands as reduction-promoting catalysts, herein, we report an efficient reduction of different aldehydes using  $NaBH_4$  and also heterogeneous oxidation of different alkenes with  $H_2O_2$  in the presence of an oxovanadium(IV) and manganese(II) Schiff base complexes encapsulated in the nanocavities of zeolite-Y.

## Experimental

### Materials

(2,4-Dihydroxyacetophenone), 1,2-diaminopropane, ethylenediamine, zeolite-Y ( $Na_{52}[(AlO_2)_52(SiO_2)_{140}]$ ), hydrogen peroxide (30 %) and sodium borohydride were obtained from Merck. Other materials were of commercial reagent grade and were purchased from Sigma-Aldrich or FLUKA companies and treated when necessary.

✉ Saeed Rayati  
rayati@kntu.ac.ir; srayati@yahoo.com

<sup>1</sup> Department of Chemistry, K. N. Toosi University of Technology, P.O. Box 16315-1618, Tehran 15418, Iran

## Physicochemical characterization techniques

NMR spectrum was recorded in  $\text{CDCl}_3$  with a Bruker FT-NMR 500 (500 MHz) spectrometer. Fourier transform infrared spectra (FTIR) were collected in an ABB Bomem FTLA 2000-100 spectrophotometer with KBr disk in the 400–4000  $\text{cm}^{-1}$  range. Ultraviolet–visible (UV–Vis) spectra were carried on the 200–700 nm range with a Lambda 25 PerkinElmer Spectrophotometer. For powder X-ray diffraction (XRD) analysis, self-oriented films were placed on neutral glass sample holders. The patterns were obtained in the reflection mode on a STOE STADIP diffractometer using monochromatized  $\text{Cu K}\alpha$  radiation as incident beam. Data were collected over the  $2\theta$  range of  $10^\circ$ – $80^\circ$ . Nitrogen sorption experiments were recorded using a Belsorp-BEL, Inc. analyzer at 77 K. The surface areas were calculated by Brunauer–Emmett–Teller (BET) method, and the pore size distributions were calculated from the adsorption branch of the isotherms using BJH method. The scanning electron microscopy (SEM) images were obtained using a VEGA3 TESCAN scanning electron microscope. The conversions of the products were accomplished by GC-FID on a Shimadzu GC-14B instrument equipped with a flame ionization detector and a SAB-5 capillary column (phenyl methyl siloxane 30 m  $\times$  320 mm  $\times$  0.25 mm). After completely destroying the zeolitic framework, vanadium and manganese percentages were analyzed by atomic absorption spectrophotometry (AAS) with flame atomization (Varian AA240).

## Preparation of the ligands

To an ethanolic solution (30 mL) of 1,2-diaminopropane (0.074 g, 1 mmol for  $\text{H}_2\text{L}_1$ ) or ethylenediamine (0.059 g, 1 mmol for  $\text{H}_2\text{L}_2$ ), 2,4-dihydroxyacetophenone (0.304 g, 2 mmol) was added. The solution was stirred and heated to reflux for 1 h. Then, obtained precipitate was filtered off and washed with warm ethanol.

Analysis calculated for bis(2,4-dihydroxyacetophenone)-1,2-propanediimine ( $\text{H}_2\text{L}_1$ )  $\text{C}_{19}\text{H}_{22}\text{N}_2\text{O}_4$  (342.16), selected FTIR data,  $\nu$  ( $\text{cm}^{-1}$ ): 3422 (O–H), 2856–2982 (C–H), 1623 (C=N), 1537 (C=C), 1052 (C–O).  $^1\text{H}$  NMR ( $\delta$ ): 1.26–1.28 (d, 3H,  $\text{NCH}_2\text{CH}(\text{CH}_3)\text{N}$ ), 2.2–2.3 (d, 6H, ( $\text{CH}_3$ ) C=N), 3.5–3.7 (m, 1H,  $\text{NCH}_2\text{CH}(\text{CH}_3)\text{N}$ ), 4.18–4.19 (m, 2H,  $\text{NCH}_2\text{CH}(\text{CH}_3)\text{N}$ ), 6.03–7.40 (m, 6H, ArH), 16.52–16.67 (s, 4H, OH). UV–Vis ( $\text{CHCl}_3$ ): 279 nm ( $\pi \rightarrow \pi^*$ ), 306 nm ( $n \rightarrow \pi^*$ ).

Analysis calculated for bis(2,4-dihydroxyacetophenone)-ethylenediimine ( $\text{H}_2\text{L}_2$ ):  $\text{C}_{18}\text{H}_{20}\text{N}_2\text{O}_4$  (328.18), selected FTIR data,  $\nu$  ( $\text{cm}^{-1}$ ): 3367 (O–H), 2856–2933 (C–H), 1633 (C=N), 1589 (C=C), 1084 (C–O).  $^1\text{H}$  NMR ( $\delta$ ): 2.2–2.3 (s, 6H, ( $\text{CH}_3$ ) C=N), 3.81 (s, 4H,  $\text{N}(\text{CH}_2)_2\text{N}$ ), 6.02–7.44 (m, 6H, ArH), 16.53 (s, 4H, OH). UV–Vis ( $\text{CHCl}_3$ ): 281 nm ( $\pi \rightarrow \pi^*$ ), 314 nm ( $n \rightarrow \pi^*$ ).

The procedures for the preparation of metal (M = Mn and VO) complexes are as follows: 1 mmol  $\text{H}_2\text{L}_1$  or  $\text{H}_2\text{L}_2$

was dissolved in 20 mL of ethanol. Ethanolic solutions of 1 mmol vanadyl acetylacetonate or manganese acetate were added to above solution, and the reaction mixture was refluxed for 2 h. The colored solution was concentrated to yield colored powders. The products were washed with warm ethanol.

M–Y was prepared by ion-exchange method: Typically, 3 g of one type of the above-mentioned metal ion was first dissolved in 100 mL deionized water. Then, 1.25 g Na–Y was added to the solution and further stirred for 24 h at  $90^\circ\text{C}$ . The solid was filtered and washed with deionized water and dried at room temperature.

Encapsulation of metal complex was performed with the flexible ligand method. M–Y (0.7 g) and 1.25 g of ligand were mixed in 50 mL of methanol, and the reaction mixture was refluxed for 17 h in an oil bath with stirring. The resulting material was separated by filtration and then extracted with methanol using Soxhlet extractor for 72 h to remove unreacted ligand from the cavities of the zeolite as well as those located on the surface of the zeolite along with neat complexes, if any. The unreacted metal ions present in the zeolite were removed by stirring with aqueous 0.01 M NaCl solution. The resulting solid was filtered and washed with distilled water until free from chloride ions. Finally, it was dried at  $120^\circ\text{C}$  in an air oven for several hours.

## Catalytic measurements

### *General procedure for catalytic oxidation of alkenes with hydrogen peroxide*

In a typical procedure, to a mixture of alkene (0.32 mmol) and catalyst (0.0008 mmol) in  $\text{CH}_3\text{CN}$  (1 mL), was added 1 mL of  $\text{H}_2\text{O}_2$ . The reaction mixture was refluxed for 4 h. The progress of the reaction was monitored by GLC.

### *General procedure for catalytic reduction of aldehydes with sodium borohydride*

To a mixture of aldehyde (0.1 mmol) and catalyst (0.003 mmol) in methanol (1 mL), 1.8 mg  $\text{NaBH}_4$  (0.05 mmol) was added. The reaction mixture was stirred magnetically at room temperature for 2 min, and the progress of the reaction was monitored by GC.

## Results and discussion

### Characterization of the catalysts

The metal-exchanged M–Y zeolite (M = Mn(II) and VO(IV)) was prepared by exchanging  $\text{Na}^+$  of the zeolite with the desired metal ion. In order to insert the Schiff base

ligands in the cavity of the zeolite, an excess amount of the ligands refluxed with M–Y zeolite in an oil bath with stirring. The percentages of metal content of various catalysts

**Table 1** Metal content of the catalysts

No.	Catalyst	Metal content (wt%)
1	MnL <sub>1</sub> -Y	4.19
2	MnL <sub>2</sub> -Y	3.14
3	VOL <sub>1</sub> -Y	2.5
4	VOL <sub>2</sub> -Y	2.6

**Table 2** IR spectral data of ligands and zeolite-encapsulated metal complexes

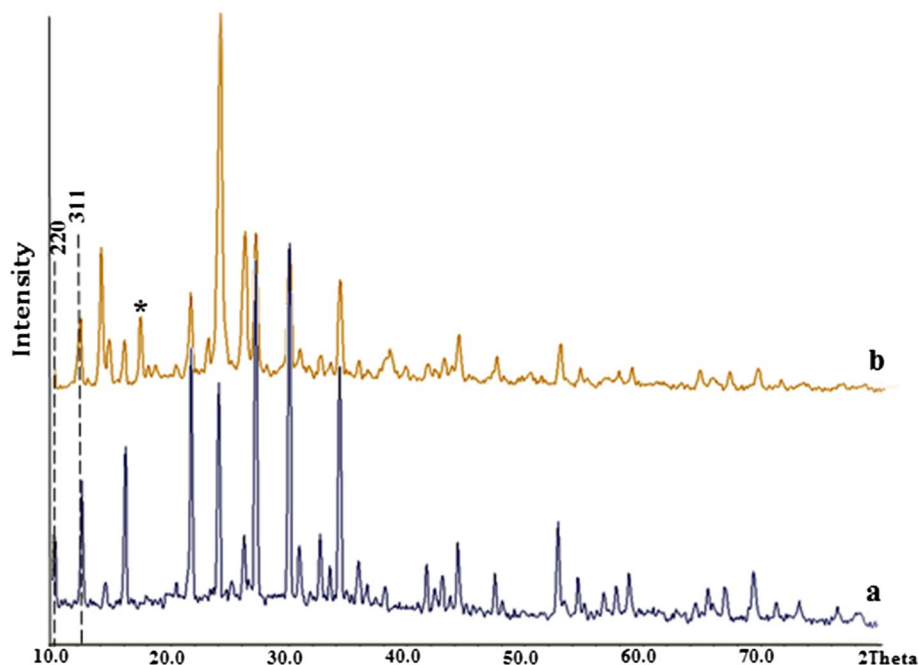
Samples	Wave number (cm <sup>-1</sup> )				
	$\nu_{(\text{Al-O-Si})}$	$\nu_{(\text{Al-O-Si})}$	$\nu_{(\text{C=C})}$	$\nu_{(\text{C=N})}$	$\nu_{(\text{O-H})}$
H <sub>2</sub> L <sub>1</sub>	–	–	1537	1623	3422
H <sub>2</sub> L <sub>2</sub>	–	–	1589	1633	3354
MnL <sub>1</sub>	–	–	1492	1614	3474
MnL <sub>2</sub>	–	–	1502	1627	3424
VOL <sub>1</sub>	–	–	1540	1614	3415
VOL <sub>2</sub>	–	–	1532	1610	3389
Mn-Y	689	1007	–	–	3219
VO-Y	691	1003	–	–	3402
MnL <sub>1</sub> -Y	796	1010	1548	1627	3424
MnL <sub>2</sub> -Y	793	1052	1555	1644	3438
VOL <sub>1</sub> -Y	793	996	1541	1634	3498
VOL <sub>2</sub> -Y	795	1057	1590	1632	3506

estimated by atomic absorption spectrometer are presented in Table 1.

The FTIR spectral data can give information regarding the crystallinity of the zeolite and the encapsulation of complexes. Comparison of the spectra of neat complexes with Schiff base ligands provides evidence for the coordinating mode of ligand in the complexes (Table 2). The sharp and strong band is observed at 1623 and 1633 cm<sup>-1</sup> due to  $\nu(\text{C=N})$  of azomethine group of the H<sub>2</sub>L<sub>1</sub> and H<sub>2</sub>L<sub>2</sub> ligands, respectively. This band is appeared at ~1614–1627 cm<sup>-1</sup> in the spectra of neat complexes and at ~1627–1644 cm<sup>-1</sup> in the spectra of encapsulated complexes that suggests the coordination of azomethine nitrogen to the metal center [17]. The phenolic –OH vibration of the Schiff base ligands H<sub>2</sub>L<sub>1</sub> (3422 cm<sup>-1</sup>) and H<sub>2</sub>L<sub>2</sub> (3354 cm<sup>-1</sup>) disappeared in that of the neat complexes, indicating the involvement of this group in coordination with the metal ion, via de-protonation.

The FTIR studies of Na–Y- and zeolite-encapsulated metal complexes show that the peak intensities are weak due to low concentration of the complexes in zeolite. In the IR spectra of the modified zeolites, a broad band in the range of 3200–3600 cm<sup>-1</sup> is attributed to the adsorbing tendency of surface hydroxyl groups, and the bands at 450–1200 cm<sup>-1</sup> are because of lattice (Si/Al)O<sub>4</sub> vibrations [18]. The asymmetric stretching and symmetric stretching of the Al–O–Si framework of the zeolite are presented in Table 2. No shift or broadening of zeolite vibrations is observed upon insertion of the complexes, which provides further evidence that the zeolite framework remains unchanged.

**Fig. 1** XRD patterns of (a) Mn-Y and (b) MnL<sub>1</sub>-Y



The powder X-ray diffraction patterns of the Mn-exchanged zeolites and the encapsulated Mn–Schiff base complex in zeolite are shown in Fig. 1.

The XRD pattern of Mn–Y-entrapped complex is similar to that of neat Mn–Y. Except the zeolite with encapsulated Mn–Schiff base has slightly weaker intensity. These observations indicate that the framework and crystallinity of the zeolite do not suffer any significant structural changes during encapsulation of the metal complex and that the complex was well distributed in the cages.

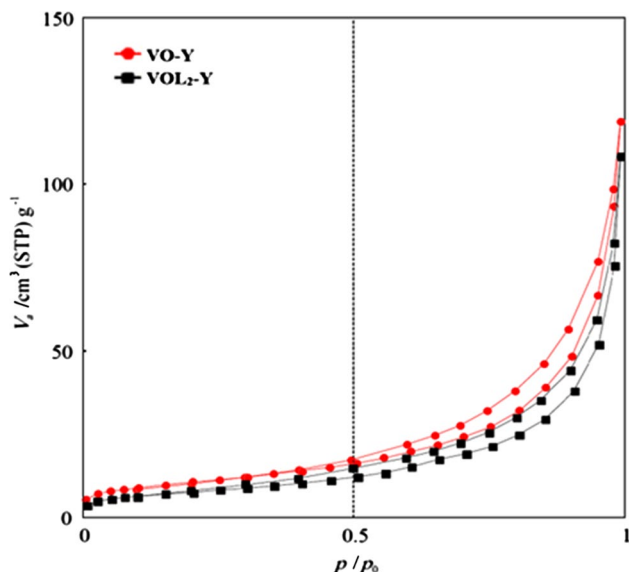
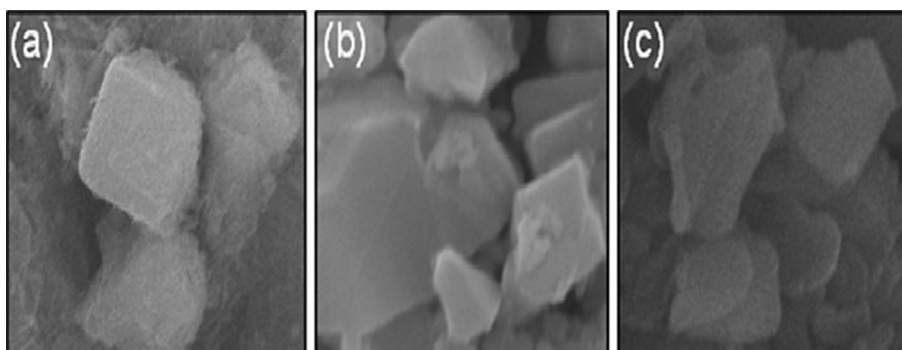


**Fig. 2**  $N_2$  adsorption–desorption isotherms corresponding to VO–Y and  $VOL_2$ –Y

**Table 3** Textural properties of VO–Y and its complex-encapsulated analogue

Sample	$S_{BET}$ ( $m^2 g^{-1}$ )	Average pore size (nm)	Pore volume ( $cm^3 g^{-1}$ )
VO–Y	106.11	24.93	0.17
$VOL_2$ –Y	72.88	23.30	0.096

**Fig. 3** SEM images of **a** Na–Y, **b**  $MnL_1$ –Y and **c**  $VOL_1$ –Y



The relative peak intensities of the 220 and 311 reflections appearing at  $2\theta = 10^\circ$  and  $12^\circ$  have been thought to be correlated with the locations of cations [19, 20]. In zeolite–Y, the peak intensity is in the order:  $I_{220} > I_{311}$  [21], while in Mn-exchanged and Mn-entrapped complex, the order of peak intensity became  $I_{311} > I_{220}$  (Fig. 1). The difference indicates that the ion  $Mn^{2+}$  exchanged which substitutes at the location of  $Na^+$ .

After careful comparison of XRD patterns of Mn–Y and  $MnL_1$ –Y, new diffraction peak was observed with  $2\theta$  values of  $17.43^\circ$  in  $MnL_1$ –Y but not observed in Mn–Y. This new peak suggests the allocation and formation of metal complex in the cavity of zeolite.

To study the textural characteristics of the encapsulated  $VOL_2$  complex in comparison with the VO–Y zeolite, nitrogen adsorption–desorption isotherms were recorded (Fig. 2).

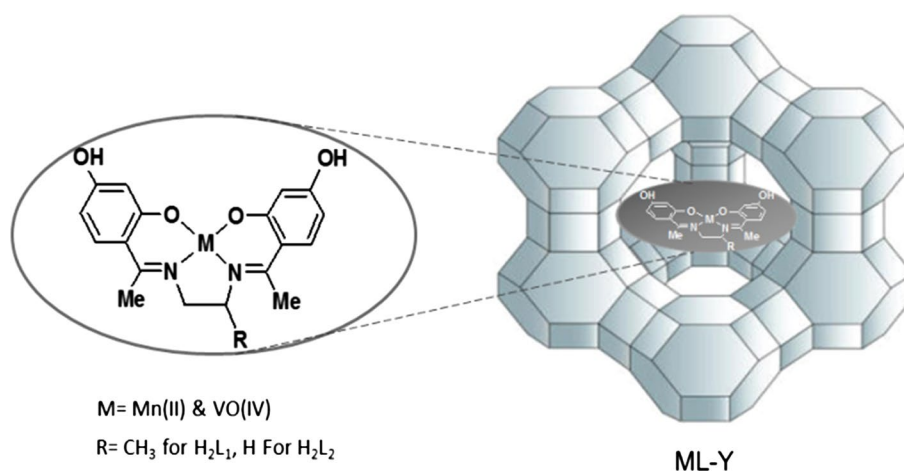
The VO–Y and  $VOL_2$ –Y present type I isotherms according to the IUPAC classification [22], showing a high uptake of nitrogen at very low relative pressures, which is characteristic of microporous nature of the materials.

Table 3 summarizes the BET surface area ( $S_{BET}$ ), the total pore volume and the average pore size of the catalyst support. The surface area of VO–Y was observed to be  $106.11 m^2 g^{-1}$ . However, in the case of  $VOL_2$ –Y, the surface area was drastically reduced to  $72.88 m^2 g^{-1}$ . The average pore size of VO–Y was 24.93 nm, and it reduced to 23.30 nm on  $VOL_2$ –Y, possibly due to the presence of metal complex in the pores of zeolite [23]. The decrease in the surface area and pore volume clearly suggests that the metal complex was encapsulated in the zeolite nanocavities.

Typical scanning electron micrographs obtained for the parent Na–Y,  $MnL_1$ –Y and  $VOL_1$ –Y are shown in Fig. 3a–c. The Na–Y has a cubic angular shape. The SEM analysis of the  $MnL_1$ –Y and  $VOL_1$ –Y shows that the crystalline nature of Na–Y remains almost the same even after complexation occurs in the cavities of zeolite.

NMR, FTIR and the above-mentioned spectral studies confirm the possible proposed structure of the complexes in the free and encapsulated systems, as given in Scheme 1.

**Scheme 1** Proposed framework structure of zeolite with encapsulated metal Schiff base complexes of Mn(II) and VO(IV)



**Table 4** Catalytic activity in epoxidation of cyclooctene over MnL<sub>1</sub>-Y under different reaction conditions

Entry	Reaction parameters	Conditions	Conversion % <sup>a</sup>
1	Solvent (dielectric constants)	CH <sub>3</sub> CN (37.5)	70
		CH <sub>3</sub> OH (32.7)	3
		C <sub>2</sub> H <sub>5</sub> OH (26.6)	2
		CH <sub>2</sub> Cl <sub>2</sub> (8.9)	0
		CHCl <sub>3</sub> (4.9)	0
2	Amount of catalyst (mg)	None	0
		1.2	70
		2.4	56
3	Amount of H <sub>2</sub> O <sub>2</sub> (mL)	None	0
		1	70
		2	70

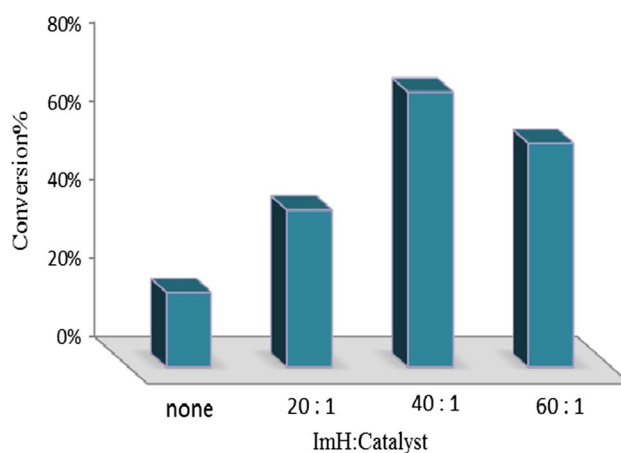
<sup>a</sup> Reaction conditions: cyclooctene (0.32 mmol), solvent (1 mL), ImH (0.032 mmol); the reactions were run for 4 h under reflux

## Catalytic activity studies

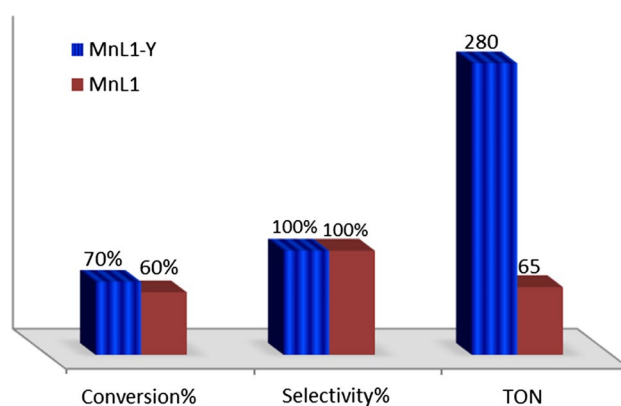
### Heterogeneous catalytic epoxidation of olefins

Epoxidation of olefins has been investigated using the encapsulated catalysts in the presence of H<sub>2</sub>O<sub>2</sub> as a green oxidant. To screen the performances of the encapsulated catalysts, MnL<sub>1</sub>-Y was chosen as the representative catalyst to study the influence of various reaction parameters to acquire maximum oxidation.

The solvent plays an important and crucial role in catalytic performance. To investigate the effect of solvent on the oxidation of cyclooctene over the MnL<sub>1</sub>-Y as catalyst, chloroform, acetonitrile, dichloromethane, methanol and ethanol were used as solvents and the highest conversion was obtained in acetonitrile (Table 4, entry 1). The solvent was changed from polar solvent (acetonitrile) to low polar solvent (chloroform) keeping other reaction conditions



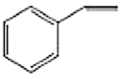
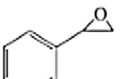
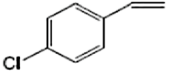
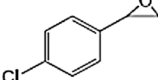
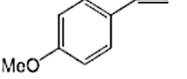
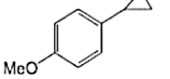
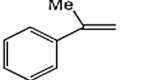
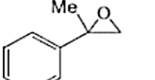
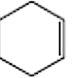
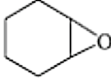
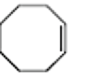
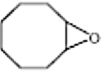
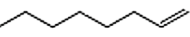
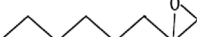
**Fig. 4** Screening of the different ImH/catalyst molar ratios on the epoxidation of cyclooctene with H<sub>2</sub>O<sub>2</sub>. See the footnote of Table 4



**Fig. 5** Screening of the epoxidation of cyclooctene by homogeneous and heterogeneous catalysts with H<sub>2</sub>O<sub>2</sub>. See the footnote of Table 4

constant. Cyclooctene conversion was found to be 70 % in acetonitrile, which decreased markedly in the CHCl<sub>3</sub> to 0 % after 4 h. This could be explained by the polarity of

**Table 5** Epoxidation of olefins using  $\text{H}_2\text{O}_2$  catalyzed by  $\text{ML}_x\text{-Y}$  ( $\text{M} = \text{Mn}$  and  $\text{VO}$ ,  $x = 1$  and  $2$ ).<sup>a</sup>

Entry	Alkenes	Product	Catalyst	Conversion % <sup>b</sup>	Selectivity %	TON <sup>c</sup>
1			$\text{MnL}_1\text{Y}$	31	100	124
			$\text{MnL}_2\text{Y}$	41	100	164
			$\text{VoL}_1\text{Y}$	6	80	30
			$\text{VoL}_2\text{Y}$	13	81	64
2			$\text{MnL}_1\text{Y}$	33	78	168
			$\text{MnL}_2\text{Y}$	23	64	144
			$\text{VoL}_1\text{Y}$	23	100	92
			$\text{VoL}_2\text{Y}$	17	100	68
3			$\text{MnL}_1\text{Y}$	100	100	400
			$\text{MnL}_2\text{Y}$	81	81	400
			$\text{VoL}_1\text{Y}$	24	72	132
			$\text{VoL}_2\text{Y}$	31	63	196
4			$\text{MnL}_1\text{Y}$	92	100	368
			$\text{MnL}_2\text{Y}$	77	78	392
			$\text{VoL}_1\text{Y}$	41	80	204
			$\text{VoL}_2\text{Y}$	41	84	196
5			$\text{MnL}_1\text{Y}$	68	100	272
			$\text{MnL}_2\text{Y}$	63	100	252
			$\text{VoL}_1\text{Y}$	43	100	172
			$\text{VoL}_2\text{Y}$	57	100	228
6			$\text{MnL}_1\text{Y}$	70	100	280
			$\text{MnL}_2\text{Y}$	63	100	252
			$\text{VoL}_1\text{Y}$	19	100	76
			$\text{VoL}_2\text{Y}$	26	100	104
7			$\text{MnL}_1\text{Y}$	4	100	16
			$\text{MnL}_2\text{Y}$	4	100	16
			$\text{VoL}_1\text{Y}$	1	100	4
			$\text{VoL}_2\text{Y}$	2	100	8

<sup>a</sup> (0.32 mmol) alkene, (1 mL)  $\text{H}_2\text{O}_2$ , (1 mL)  $\text{CH}_3\text{CN}$ , (4 h) time, under reflux

<sup>b</sup> Conversions and selectivities were determined by GC based on the starting alkene

<sup>c</sup> TON: (total turnover number) the ratio of the number of moles of product to the number of moles of catalyst

the used solvent [24]. The higher conversions in acetonitrile (70 % with  $\text{H}_2\text{O}_2$ ) relative to the others possibly may be due to the higher boiling point of acetonitrile.

To test the influence of the amount of the catalyst on the catalytic reactivity of cyclooctene epoxidation, various amounts of catalyst were used and compared. In the absence of the catalyst (Table 4, entry 1), the reactions did not proceed under reflux. The highest conversion of cyclooctene was obtained with 1.2 mg of catalyst and further increase in the amount of catalyst to 2.4 mg, the % cyclooctene conversion decreased to 56 %. This is may be due to faster decomposition of  $\text{H}_2\text{O}_2$  in the presence of excess of the catalyst [25].

Different oxidant ( $\text{H}_2\text{O}_2$ ) concentrations have been studied in the oxidation of cyclooctene (Table 4, entry 3). In the absence of oxidant, no activity is observed and the oxidation of cyclooctene required 1 mL of  $\text{H}_2\text{O}_2$  for completion. Further addition of  $\text{H}_2\text{O}_2$  to the reaction mixture led to similar results.

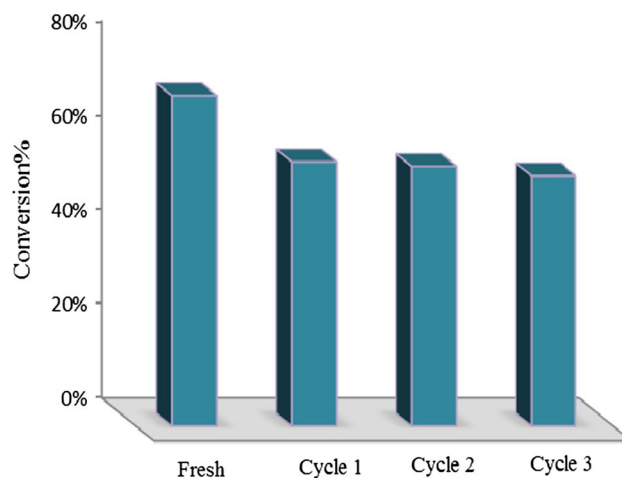


**Fig. 6** Results obtained in the epoxidation of cyclooctene with  $\text{H}_2\text{O}_2$  by  $\text{MnL}_1\text{-Y}$  with a catalyst reused several times. Reaction conditions: cyclooctene (0.32 mmol), solvent (1 mL),  $\text{H}_2\text{O}_2$  (1 mL); the reactions were run for 4 h under reflux



The reactivity of manganese catalysts in the oxidation reactions can be improved by the addition of different nitrogenous bases as co-catalyst [26–28]. For a better understanding of the role of the imidazole in this catalytic system, the effect of different molar ratios of the ImH/catalyst on the epoxidation of cyclooctene was investigated. In the absence of imidazole, the reaction proceeds only in 19 % yield, whereas the addition of imidazole increased the reaction conversion (Fig. 4).

An increase in the ImH/catalyst molar ratio up to 40 remarkably improved the reaction rate. Beyond this ratio, a significant decrease in catalytic efficiency is observed, which may be attributed to the formation of an inactive species [29].

In order to demonstrate the effect of encapsulation of the catalysts in the nanocavities of the zeolite-Y, on the catalytic activity of manganese (III) Schiff base complexes in the oxidation reactions, the epoxidation of cyclooctene with  $\text{H}_2\text{O}_2$  was carried out in the presence of neat  $\text{MnL}^{\text{I}}$  and  $\text{MnL}^{\text{I}}\text{-Y}$  in a comparative manner (Fig. 5).

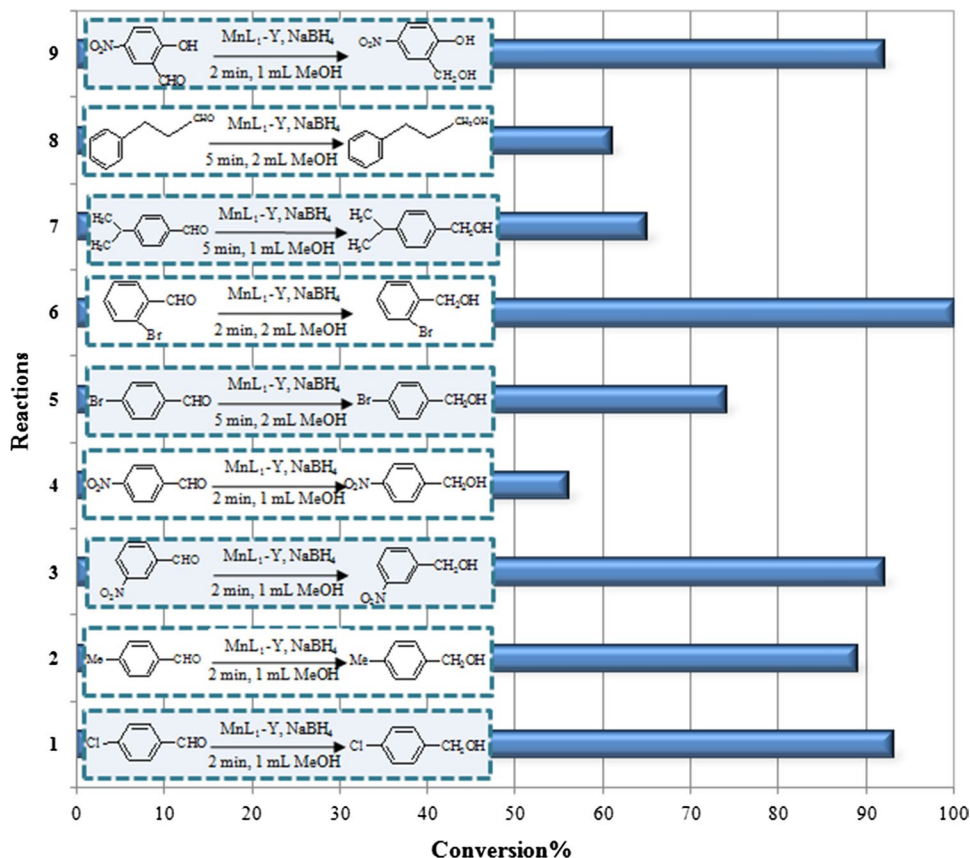
The encapsulated catalyst was more active than the corresponding neat complex, and the turnover number (TON) increases dramatically in the Mn–Schiff base complex into the zeolite-Y. Also oxidation of cyclooctene in the presence of neat  $\text{VOL}_1$  led to the formation of 30 % cyclooctene oxide as the sole product.

In order to verify the catalytic scope of this catalytic system, under optimized conditions, it has also been applied for epoxidation of a wide variety of alkenes (Table 5). It was obvious that this catalyst ( $\text{MnL}_1\text{-Y}$ ) could efficiently convert 4-methoxystyrene,  $\alpha$ -methylstyrene, cyclooctene and cyclohexene to their corresponding epoxides. However, catalytic epoxidation of styrene and 4-chlorostyrene was found less efficient. The terminal linear alkene (1-octene) was null reaction. Because of the low  $\pi$ -electron density of linear terminal alkene, they are less reactive toward electrophiles than internal alkenes [30]. Much reactivity observed in the case of  $\text{MnL}_1\text{-Y}$  in comparison with  $\text{MnL}_2\text{-Y}$  seems to be due to its higher concentration of the manganese catalyst in the nanocavities of the zeolite-Y (Table 1).

The effect of transition metal complexes encapsulated in zeolite,  $\text{ML}_x\text{-Y}$  ( $\text{M} = \text{Mn(II)}$  and  $\text{VO(IV)}$ ,  $x = 1$  and  $2$ ), was studied on the epoxidation of variety of alkenes with hydrogen peroxide, and the results are shown in Table 5. It is clear from results that manganese complexes encapsulated in zeolite are more active than vanadium complexes.

The reusability of a heterogeneous catalyst is of great importance in catalyst design. The homogeneous  $\text{MnL}_1$  is readily degraded and cannot be recovered even once; in contrast, the supported manganese Schiff base

**Fig. 7** Reduction of aldehydes with  $\text{NaBH}_4$  in the presence of  $\text{MnL}_1\text{-Y}$  in methanol at room temperature; Reaction conditions: the molar ratios for catalyst/substrate/ $\text{NaBH}_4$  are 1:30:15



catalyst can be filtered and reused several times without significant loss of its activity. The reusability of  $MnL_1-Y$  catalyst was tested over three consecutive runs, and the consequent results are illustrated in Fig. 5. The used catalyst was recovered and rinsed with copious amount of methanol after each catalytic run. The washed catalyst was dried at 110 °C for 24 h before reuse. The catalytic activity after the first cycle of  $MnL_1-Y$  has an obvious decrease compared with the fresh catalyst (Fig. 6).

This decrease in activity is also accompanied with an apparent decrease in the amount of manganese content.

#### Heterogeneous catalytic reduction of aldehydes

The high catalytic activity of  $MnL_1-Y$  in the oxidation of alkenes prompted us to explore its catalytic activity in the reduction of aromatic aldehydes to their corresponding alcohols with sodium borohydride at room temperature (Fig. 7).

Results in Fig. 7 showed that in the presence of this catalyst, high-to-excellent conversions (56–100 %) were obtained for most of the aldehydes. While the reduction of 4-chlorobenzaldehyde in the presence of  $MnL_1-Y$  led to 93 % reduction of the aldehyde (reaction 1 in Fig. 7), running the reaction in the absence of the catalyst gave the product with a yield of 25 %.

As shown in Fig. 8, transition metal complexes encapsulated in zeolite;  $ML_x-Y$  ( $M = Mn(II)$  and  $VO(IV)$ ,  $x = 1$  and 2) could be advantageously used as catalyst in reduction of 4-methylbenzaldehyde.

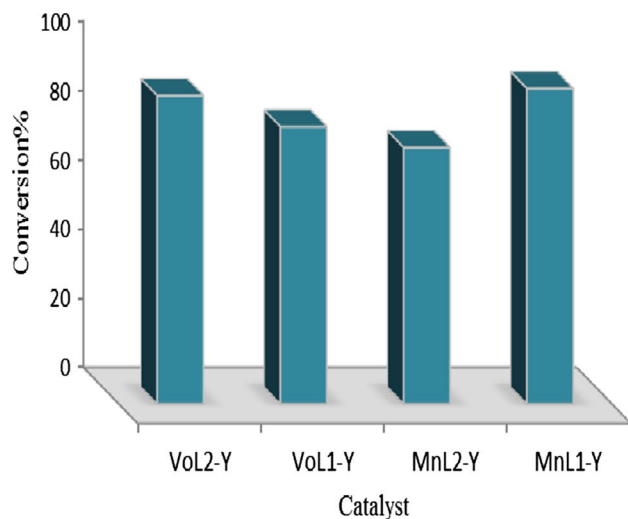


**Fig. 8** Reduction of 4-methylbenzaldehyde with  $NaBH_4$  in the presence of  $ML_x-Y$  ( $M = Mn(II)$  and  $VO(IV)$ ,  $x = 1$  and 2) in methanol at room temperature; See the figure caption of Fig. 7

## Conclusion

It can be concluded that  $ML_x$  ( $M = Mn(II)$  and  $VO(IV)$ ,  $x = 1$  and 2) complexes can be encapsulated in Na-Y zeolite supercages without structural modification or loss of crystallinity of the zeolite framework. The physicochemical studies confirmed the encapsulation of metal complexes in the supercages of zeolite-Y. Catalytic activity of the prepared catalysts in both oxidation of alkenes with  $H_2O_2$  and reduction of aldehydes with  $NaBH_4$  was investigated. In the both catalytic reactions, manganese complexes show higher catalytic activity than the vanadium ones.

**Acknowledgments** This work has been supported by the Iran National Science Foundation (INSF) (Grant No. 88001216).

## References

- D.J. Xuereb, R. Raja, *Catal. Sci. Technol.* **1**, 517 (2011)
- M.L. Cano, A. Corma, V. Fornes, H. García, M.A. Miranda, C. Baerlocher, C. Lengauer, *J. Am. Chem. Soc.* **118**, 11006 (1996)
- R.J. Corrêa, G.C. Salomao, M.H.N. Olsen, L.C. Filho, V. Drago, C. Fernandes, O.A.C. Antunes, *Appl. Catal. A* **336**, 35 (2008)
- J. Poltowicz, K. Pamin, E. Tabor, J. Haber, A. Adamski, Z. Sojka, *Appl. Catal. A* **299**, 235 (2006)
- S. Rayati, F. Salehi, *J. Iran. Chem. Soc.* **12**, 309 (2015)
- G. Reddy, S. Balasubramanian, K. Chennakesavulu, *J. Mater. Chem. A* **2**, 15598 (2014)
- M. Salavati-Niasari, M. Shakouri-Arani, F. Davar, *Microporous Mesoporous Mater.* **116**, 77 (2008)
- C.K. Modi, B.G. Gade, J.A. Chudasama, D.K. Parmar, H.D. Nakum, A.L. Patel, *Acta Part A Mol. Biomol. Spectrosc.* **140**, 174 (2015)
- G.J. Kim, D.W. Park, Y.S. Tak, *Catal. Lett.* **65**, 127 (2000)
- T. Yamada, T. Nagata, K.D. Sugi, K. Yoroze, T. Ikeno, Y. Ohtsuka, D. Miyazaki, T. Mukaiyama, *Chem. Eur. J.* **9**, 4485 (2003)
- G.J. Kim, J.H. Shin, *Catal. Lett.* **63**, 205 (1999)
- W. Kahlen, H.H. Wagner, W.F. Holderich, *Catal. Lett.* **54**, 85 (1998)
- W. Kahlen, A. Johnson, W.F. Holderich, *Stud. Surf. Sci. Catal.* **108**, 469 (1997)
- S. Rayati, P. Abdolalian, C. R. Chimie. **16**, 814 (2013)
- M. Navidi, B. Movassagh, S. Rayati, *Appl. Catal. A Gen.* **452**, 24 (2013)
- S. Rayati, N. Rafiee, A. Wojtczak, *Inorg. Chimica Acta* **368**, 27 (2012)
- C.K. Modi, D.H. Jani, *J. Therm. Anal. Calorim.* **102**, 1001 (2010)
- S.M. Emam, F.A.E. Saied, S.A.E. Enein, H.A.E. Shater, *Spectrochim. Acta Part A* **72**, 291 (2009)
- W.H. Quayle, J.H. Lunsford, *Inorg. Chem.* **21**, 97 (1982)
- W.H. Quayle, G. Peeters, G.L. DeRoy, E.F. Vansant, J.H. Lunsford, *Inorg. Chem.* **21**, 2226 (1982)
- H.S. Abbo, S.J.J. Titinchi, *Top. Catal.* **53**, 254 (2010)
- K.S.W. Sing, D.H. Everett, R.A.W. Haul, L. Moscou, R.A. Pierotti, J. Rouquerol, T. Siemieniowska, *Pure Appl. Chem.* **57**, 603 (1985)
- K.J. Balkus Jr., A.G. Gabrielov, *J. Incl. Phenom. Mol. Recognit. Chem.* **21**, 159 (1995)
- A. Corma, P. Esteve, A. Martinez, *J. Catal.* **161**, 11 (1996)



25. R.A. Sheldon, J.K. Kochi, *Metal-Catalyzed Oxidation of Organic Compounds* (Academic Press, New York, 1981)
26. A. Ghaemi, S. Rayati, S. Zakavi, N. Safari, *Appl. Catal. A Gen.* **353**, 154 (2009)
27. S. Rayati, S. Zakavi, V. Noroozi, S.H. Motlagh, *Catal. Commun.* **10**, 221 (2008)
28. S. Rayati, S. Zakavi, S.H. Motlagh, V. Noroozi, M. Razmjoo, A. Wojtczak, A. Kozakiewicz, *Polyhedron* **27**, 2285 (2008)
29. A.D. Adler, F.R. Longo, F. Kampas, J. Kim, *J. Inorg. Nucl. Chem.* **32**, 2443 (1970)
30. K. Tong, K. Wong, T. Chan, *Org. Lett.* **5**, 3423 (2003)